

AD-A208 448

Frequency Division Multiplexing of Interferometric Sensor Arrays

A. DANDRIDGE, A. B. TVETEN, A. M. YUREK, A. D. KERSEY AND E. C. MCGARRY*

*Optical Techniques Branch
Optical Sciences Division*

**Sachs/Freeman Associates
1401 McCormick Drive
Landover, MD 20785*

May 3, 1989

DTIC
ELECTE
JUN 05 1989
S E & D

Approved for public release; distribution unlimited.

1 89 6 05 008

SECURITY CLASSIFICATION OF THIS PAGE

REPORT DOCUMENTATION PAGE				Form Approved OMB No 0704-0188	
1a REPORT SECURITY CLASSIFICATION UNCLASSIFIED			1b RESTRICTIVE MARKINGS		
2a SECURITY CLASSIFICATION AUTHORITY		3 DISTRIBUTION/AVAILABILITY OF REPORT Approved for public release; distribution unlimited.			
2b DECLASSIFICATION/DOWNGRADING SCHEDULE					
4 PERFORMING ORGANIZATION REPORT NUMBER(S) NRL Memorandum Report 6457			5 MONITORING ORGANIZATION REPORT NUMBER(S)		
6a NAME OF PERFORMING ORGANIZATION Naval Research Laboratory		6b OFFICE SYMBOL (if applicable) Code 6574	7a NAME OF MONITORING ORGANIZATION		
6c ADDRESS (City, State, and ZIP Code) Washington, DC 20375-5000			7b ADDRESS (City, State, and ZIP Code)		
8a NAME OF FUNDING/SPONSORING ORGANIZATION NUSC		8b OFFICE SYMBOL (if applicable)	9 PROCUREMENT INSTRUMENT IDENTIFICATION NUMBER		
8c ADDRESS (City, State, and ZIP Code) Arlington, VA		10 SOURCE OF FUNDING NUMBERS			
		PROGRAM ELEMENT NO	PROJECT NO	TASK NO	WORK UNIT ACCESSION NO
11 TITLE (Include Security Classification) Frequency Division Multiplexing of Interferometric Sensor Arrays					
12 PERSONAL AUTHOR(S) (See page ii)					
13a TYPE OF REPORT		13b TIME COVERED FROM 10/1/86 TO 9/31/87	14 DATE OF REPORT (Year, Month, Day) 1989 May 3		15 PAGE COUNT 33
16 SUPPLEMENTARY NOTATION *Sachs/Freeman Associates, 1401 McCormick Drive, Landover, MD 20785					
17 COSATI CODES			18 SUBJECT TERMS (Continue on reverse if necessary and identify by block number)		
FIELD	GROUP	SUB-GROUP	Fiber optic sensors		
			Frequency division multiplexing		
			Interferometric sensor arrays		
19 ABSTRACT (Continue on reverse if necessary and identify by block number) This report demonstrates the multiplexing of fiber optic interferometric sensors using a CW phase generated carrier technique. The technique employs modulated diode laser sources at different carrier frequencies, near balanced interferometers (≈ 4 cm path difference) and phase generated carrier demultiplexing demodulation. This approach leads to a simple all-passive sensor array which has intrinsically low crosstalk. The system is analyzed in terms of shot noise performance and crosstalk. An experimental all optical implementation of a four sensor array was demonstrated; both the single sensor and multisensor arrays were limited by the laser phase noise to a sensitivity of $\sim 18 \mu\text{rad}/\sqrt{\text{Hz}}$. Crosstalk between individual channels was better than -60 dB. In the absence of laser phase noise the demodulator/demultiplexer demonstrated $\sim 2 \mu\text{rad}$ performance with both single sensor and four element array operation, and $4 \mu\text{rad}$ performance with 8 elements in operation. <i>Frequency division multiplexing (FD-M) (9.1 Hz).</i>					
20 DISTRIBUTION/AVAILABILITY OF ABSTRACT <input checked="" type="checkbox"/> UNCLASSIFIED/UNLIMITED <input type="checkbox"/> SAME AS RPT <input type="checkbox"/> DTIC USERS			21 ABSTRACT SECURITY CLASSIFICATION UNCLASSIFIED		
22a NAME OF RESPONSIBLE INDIVIDUAL Aileen M. Yurek			22b TELEPHONE (Include Area Code) (202) 767-9341		22c OFFICE SYMBOL Code 6574

DD Form 1473, JUN 86

Previous editions are obsolete

S/N 0102-LF-014-6603

SECURITY CLASSIFICATION OF THIS PAGE

SECURITY CLASSIFICATION OF THIS PAGE

12. PERSONAL AUTHORS

Dandridge, A., Tveten, A.B., Yurek, A.M., Kersey, A.D. and McGarry,* E.C.

CONTENTS

I.	INTRODUCTION	1
II.	ARRAY TOPOLOGY AND DEMODULATION	4
III.	EXPERIMENTAL SECTION	7
IV.	DISCUSSION	10
V.	SUMMARY	13
	ACKNOWLEDGEMENT	14
	REFERENCES	15

Accession For	
NTIS GPA&I	<input checked="" type="checkbox"/>
DTIC TAB	<input checked="" type="checkbox"/>
Unannounced	<input type="checkbox"/>
Justification	
By _____	
Distribution/	
Availability Codes	
Dist	Avail and/or Special
A-1	



FREQUENCY DIVISION MULTIPLEXING OF INTERFEROMETRIC SENSOR ARRAYS

I. Introduction

Since the early experiments in the late seventies, interferometric fiber optic sensors have been configured to detect many different fields¹. A number of fiber interferometric sensors have been successfully packaged and tested; these systems have employed pigtailed semiconductor diode lasers². They have displayed high sensitivity and wide dynamic range with a typical phase sensitivity of $\sim 1-3 \mu\text{rad}/\sqrt{\text{Hz}}$ at 1 KHz. Some of these sensors may be configured as single stand-alone sensors, where the sensor is in close proximity to the source and processing electronics (e.g. magnetic sensor)³. However, there has been increasing interest in passive sensors located remotely from the source and electronics. Furthermore, for applications where arrays of sensors are required, the multiplexing of fiber sensors will result in significant cost reductions. There have been a number of different approaches to sensor multiplexing, the approaches may be described as forms of coherence, time, and frequency division multiplexing.

The coherence multiplexed system requires a sensing and a receiving interferometer, the latter being near the source/detector electronics module, with the sensor remotely located. The technique requires that the path imbalance of each sensor be significantly greater than the coherence length of the source⁴. The phase information on the sensor is recovered by balancing

Manuscript approved February 24, 1989.

the path differences of the sensing and receiving interferometers. Even though each interferometer has a path imbalance longer than the coherence length of the source, the coherence of the laser is still finite at these large path imbalances. This leads to sizable phase induced intensity noise in these coherence multiplexed systems⁵. Early results where one sensor was "multiplexed" led to noise levels of $\sim 4 \text{ mrad}/\sqrt{\text{Hz}}$ ⁶. However, by combining coherence multiplexing with frequency modulation of the laser diode, the phase induced intensity noise from the unbalanced paths is upconverted out of the signal band. Interrogation of single sensors using this technique led to interferometer noise of $\sim 45 \text{ } \mu\text{rad}/\sqrt{\text{Hz}}$ ⁷, but two multiplexed sensors operating in this mode led to noise levels of 70 and 100 $\mu\text{rad}/\sqrt{\text{Hz}}$ ⁸. This performance and the fact that each sensing interferometer must have a different path length imbalance as well as its own receiving interferometer, plus the relatively long coherence length of good semiconductor diode lasers, requires excessive lengths of fiber to be employed. These drawbacks would indicate that this technique will have only limited utility.

Time division multiplexing has received considerable attention from a number of different laboratories. This technique can be separated into two approaches, one using unbalanced interferometers and long coherence length sources^{9,10}, and another, similar to coherence multiplexing, using unbalanced sensing and receiving interferometers to form a balanced system. Although this latter approach is similar in appearance to coherence multiplexing, in this technique all the sensing elements have the same path imbalance; and, due to the time division utilized, only one receiving interferometer is required. Various array topologies are employed to provide the necessary time delay between sensors. Technological difficulties prohibit direct pulsing of the

diode laser, consequently an electro optical modulator of some sort (typically a Bragg cell) is required. In the unbalanced approach, the long coherence length laser may be gated such as to provide pulses with two different frequency shifts; this allows the overlapping signal pulses generated by the interferometric elements to produce a heterodyne signal. It appears unlikely that this approach will provide good noise performance with semiconductor lasers because of strong phase induced intensity noise contributions and source coherence problems. Demonstrations of time division multiplexing with the balanced system, which allows the gating out of the noise from the unbalanced paths have provided respectable noise performance of $40 \mu\text{rad}/\sqrt{\text{Hz}}$, for a two element array¹¹. In general, although crosstalk between sensors in these systems has not been well characterized, most configurations should allow better than -40 dB crosstalk. An exception to this is the approach which employs Fabry-Perot sensors^{9;10,12}, in which higher order reflections will result in moderately severe crosstalk. The Fabry-Perot technique appears to have limited array applications because of this problem.

Although frequency division multiplexing has received some attention, this approach appears to have limited (but possibly useful) applications. Approaches using the frequency ramped continuous wave technique (FMCW) lead to substantial phase-induced intensity noise; demonstrations of single element systems indicate $200 \mu\text{rad}/\sqrt{\text{Hz}}$ performance when large path imbalances are employed¹³. Recently, multiplexing using this technique indicated performance in the $1.0 \text{ mrad}/\sqrt{\text{Hz}}$ range¹⁴. Another multiplexing technique which employs direct modulation of a non-linear transduction mechanism at the sensor results in good performance ($10 \mu\text{rad}/\sqrt{\text{Hz}}$ noise performance with three sensors)¹⁵. Although this approach may be implemented so as to provide the modulation via

a multimode link¹⁵, it requires $(N+2)$ fiber leads per N elements and thus does not reduce the fiber lead count; however, many low bandwidth sensors may be operated within a single interferometer¹⁶.

In this work we employ a frequency division multiplexing technique based on a phase generated carrier approach using direct current sinusoidal modulation of a semiconductor diode laser in conjunction with a slightly unbalanced (~ 4 cm) interferometer¹⁷. By using sources modulated at different frequencies ($\Delta f \sim 50$ kHz) a number of signals may be applied to a single return fiber. The demultiplexing is achieved by using the same circuitry used in the demodulation of a single sensor. Essentially, the components of the fundamental and second harmonic of each of the modulation frequencies are electronically mixed down to the baseband; this effectively narrow band filters each sensor output. The signals from each of the sensors are then demodulated by a differentiate-cross-multiplication technique¹⁷. In the following section the array configuration will be described and the theory of this approach will be discussed. The discussion will include elements which contribute to the signal to noise ratio as well as to the sensor crosstalk. In Section III the performance of a four and eight channel multiplexed arrays will be presented.

II. Array Topology and Demodulation

Figure 1 shows matrix representation of the proposed multiplexing scheme. The $J \times K$ array is powered by J optical sources and the sensor outputs are multiplexed onto K output fibers. The total number of sensor elements N_0 is $J \times K$ (assuming the configuration is not under-utilized). It is a trivial matter to show that a symmetrical array gives rise to the maximum multiplexing gain (i.e., the number of elements/total number of input and output fibers),

and this paper will be concerned only with this particular case (i.e., JxJ matrix). It is, however, worth pointing out that our analysis indicates that certain skewed arrays give rise to improved phase detection sensitivities at the cost of a slightly reduced multiplexing gain.

The actual optical fiber 'circuit' required for the implementation of a 16 element (4x4) array is shown in Figure 2. The Figure shows 16 sensors S_{11} , S_{12} , ... S_{44} driven by the lasers 1,2,3,4 and detected by the detectors 1,2, 3, 4, the notation is such that each sensor S_{ij} is driven by source i and detected by detector j .

Each of the sensors consist of an unbalanced interferometer, such that when the frequency of the laser is varied the phase difference between the arms of the interferometer changes. The output intensity of a single interferometer can be expressed as

$$I = A + B \cos \theta(t) \quad (1)$$

where the constants A and B are proportional to the input optical power and depend on the mixing efficiency of the interferometer. If a sinusoidal signal $C \cos \omega t$ is applied to the driving laser this will produce an output

$$I = A + B \cos [C \cos \omega t + \phi(t)] \quad (2)$$

The constant C is determined by the variation of the optical frequency with the current (dv/di) of the laser, the amplitude of the current modulation and the optical path length difference in the interferometer. The time dependent function $\phi(t)$ contains not only the signal of interest but also any environmentally induced phase shifts. The current induced amplitude variation of the laser output is ignored here for simplicity, measurements (see Experimental section) indicated that errors due to this term were less than

0.5 dB for the experimental configuration employed. Expanding equation (2) in terms of Bessel functions produces

$$I = A + B\left\{ [J_0(C) + 2 \sum_{i=1}^{\infty} (-1)^k J_{2k}(C) \cos 2k\omega t] \cos \phi(t) - [2 \sum_{k=0}^{\infty} (-1)^k J_{2k+1}(C) \cos((2k+1)\omega t)] \sin \phi(t) \right\} \quad (3)$$

Each laser being driven in the array shown in Figure 1 will produce an output similar to that in equation (3) for each interferometer. The constants A, B, and C depend on the individual interferometer and the laser characteristics, and $\phi(t)$ is the actual signal detected. As each output fiber carries signals from interferometers powered by each of the sources, to discriminate between these signals each laser needs to be driven at a different frequency to allow the signals to be separated by the electronics. The total intensity on each detector (j) is

$$I_j = \sum_{i=1}^J I_{ij} \\ = \sum_{i=1}^J \left\{ A_i + B_{ij} [J_0(C_{ij}) + 2 \sum_{k=1}^{\infty} (-1)^k J_{2k}(C_{ij}) \cos 2k\omega_i t] \cos \phi_{ij} - [2 \sum_{k=0}^{\infty} (-1)^k J_{2k+1}(C_{ij}) \cos((2k+1)\omega_i t)] \sin \phi_{ij} \right\} \quad (4)$$

Here, the sum is over the number of lasers driving the array. This intensity signal is demultiplexed by phase sensitive detection of each of the signals at ω_i and $2\omega_i$. Figure 3 shows a block diagram of such a demultiplexer. For each sensing interferometer the demultiplexer produces two outputs, one containing $\sin \phi_{ij}(t)$ and the other $\cos \phi_{ij}(t)$. A complete array would have at this point $2 \sqrt{N_0}$ output signals. These $\sin \phi_{ij}(t)$ and $\cos \phi_{ij}(t)$ signals can be demodulated in a number of ways to produce the actual signal $\phi_{ij}(t)$. The

method used in this paper was the differentiate and cross multiply approach; it is completely described in Reference 17.

As can be seen from equation (4) this type of demultiplexing scheme requires $\sqrt{N_0}$ different driving frequencies, $f_i (= \omega_i/2\pi)$. The separation between the frequencies is determined by the bandwidth of interest and a buffer band. The buffer band is determined by the frequency response of the sensor, and/or the frequency spectrum of the sensed field. In this demultiplexing system both f_i and $2f_i$ are used. This requires that all of the frequencies used be no closer than some band separation Δf . If there are $\sqrt{N_0}$ output channels arranged such that twice the highest frequency is Δf away from threetimes the lowest frequency then a formula to determine the lowest frequency (f_0) usable without overlap is given by

$$2(f_0 + (\sqrt{N_0} - 1)\Delta f) = 3f_0 - \Delta f \quad (5)$$

i.e., $f_0 = (2\sqrt{N_0} - 1) \Delta f$.

Owing to the decrease in dv/di with modulation frequency, it is necessary to modulate the laser at as low a frequency as possible to avoid excessive current excursion or interferometer path imbalance. A typical example for $\Delta f = 4\text{KHz}$ and $N_0 = 1024$ (i.e. 32×32) elements would lead to a lowest usable frequency of 252 KHz, with a maximum value of 376 KHz. A number of semiconductor laser diodes display of dv/di between 1.5 to 4 GHz/mA at 500 KHz;¹⁸ these values are sufficient for most applications.

III. Experimental Section

To demonstrate this multiplexing/demultiplexing approach, the network shown in Figure 4 was constructed. The interferometers and combining network were constructed with Allied Amphenol fiber optic couplers. Each

interferometer had approximately 2m of fiber in each arm, the fiber in one arm of each of the interferometers was wrapped around a PZT cylinder to allow test signals to be applied to each interferometer. Each interferometer had a measured path difference of 4 cm (i.e. ~ 6 cm OPD). The average loss of each fusion splice/coupler was ~ 0.5 dB; the whole system was made from the coupler fiber. The optical sources were Hitachi HLP 1400 lasers operating at $\lambda \sim 830$ μm . To test the accuracy of the path differences in each of the four sensors, another HLP 1400 was coupled into the second output port (A in figure 4) and the outputs of the four interferometers were simultaneously measured at the second input port. The laser was then current modulated to provide a modulation of the optical frequency. The four outputs indicated that the interferometers had similar path differences to within $\sim 5\%$. This also demonstrated the ability to power multi-sensor elements from a single source, which comprises one part of the proposed sensor network.

To demonstrate the actual multiplexing, the four sources (shown in Fig. 4) were modulated at the following frequencies: 40 KHz, 44 KHz, 48 KHz and 52 KHz. The lasers, whose thresholds were ~ 60 mA, were driven at a bias current of ~ 90 mA. The ac current modulation was ~ 1.5 mA rms which resulted in a phase shift $C = 2.6$ rad peak in each interferometer (i.e., $J_1(C) = J_2(C)$)¹⁷. The optical output of the combining network was detected by a Si photodetector, the power level (average) of each sensor was ~ 6 μW , this level was chosen to be a representative power value for fairly large arrays, and was achieved by reducing the input coupling to the fiber (~ 50 μW was obtainable at the outputs with optimum coupling). The output was then fed as the common input to the four demultiplexer/demodulator circuits. This output is shown in Fig. 5, the spectrum analyzer was offset by 10 KHz to allow both

the ω and 2ω carrier bands to be shown. Each of the carriers in the ω and 2ω bands was set to be equal in amplitude to ± 2 dB, via control of the laser bias current.

The noise level of each one of the four laser/sensor configurations was tested individually (i.e., only one source on at a time). Two spectrum analyzers were used to analyze the demodulated output, a Tektronix 7L5 to display the full sensor bandwidth (0-2KHz) and a Hewlett-Packard 3582A operated with higher resolution to accurately determine the noise level close to the 1 kHz test signal. All measurements of the minimum detectable noise floor are only quoted to an accuracy ± 1 dB, i.e. $\pm 10\%$. Each of the four laser/sensor/demodulator combinations indicated a noise level corresponding to 18 ± 2 $\mu\text{rad}/\sqrt{\text{Hz}}$ at 1 KHz, this is an equivalent laser frequency jitter of 14 ± 2 kHz/ $\sqrt{\text{Hz}}$, which is typical for this type of laser⁵. The demodulated output of one sensor, denoted as sensor S_1 , is shown in Fig. 6, the steep rise in the noise and the discrete peaks at low frequency were due to acousto-mechanical pickup by the interferometers which were operated in a normal open laboratory environment. The small decrease in noise at higher frequencies is due to the $1/f$ frequency dependence of the laser's frequency noise. To calibrate the demodulated output a test signal of ~ 0.05 rad (rms) was applied to the interferometer (S_1) at 1 kHz. To test whether the presence of the optical outputs of the other interferometers (denoted S_2 , S_3 and S_4) on the small fiber would degrade the performance of sensor S_1 , the lasers powering S_2 , S_3 and S_4 were switched on and modulated such that the input to A's demodulator resembled the spectrum of Fig. 5. The resultant output is also shown in Fig. 6a, as can be seen the two traces overlap to the extent that they cannot be distinguished. Thus, the increase in noise due to the presence of the other

sensor outputs is estimated to be less than 1 dB, the noise floor was again estimated to be $18 \pm 2 \mu\text{rad}/\sqrt{\text{Hz}}$. A second important point is that the demodulated output was constant to within ± 0.5 dB.

Another important parameter in defining the performance of a multiplexing scheme is that of crosstalk. To measure this the demodulated output of sensor S_1 was recorded, with S_2 , S_3 and S_4 running, this is shown in the upper trace of Figure 6b (i.e., identical to the two traces of Fig. 6a). The ~ 0.05 rad signal was then removed from S_1 and applied to S_2 while still monitoring the output of S_1 , the observed crosstalk was less than -60 dB. This result was then repeated for sensors S_3 and S_4 with similar results. Then while monitoring the output of sensor S_1 with no applied test signal, ~ 0.05 rad signals were applied simultaneously to sensors S_2 , S_3 and S_4 , this output is the lower trace of Figure 6b, the resultant crosstalk had an average value of less than -55 dB. The crosstalk appeared to be electronic in origin.

IV. Discussion

To further characterize this demultiplexing approach, it was necessary to test the system in the absence of the laser phase noise which produced the $10 \mu\text{rad}$ noise floor. In order to accomplish this, the interferometers were electronically simulated using cosine/sine generators. Recently trigonometric function generators capable of high accuracy over an extended range have become available which are ideally suited for the simulation of interferometer outputs¹⁸. The noise floor of the Analog Devices 639 chip used to simulate the interferometer noise floor was $\sim 0.3 \mu\text{rad}/\sqrt{\text{Hz}}$ at frequencies above 20 Hz. This low noise allows measurement of the demultiplexer and demodulator noise floors, without being contaminated by laser noise. Four of these synthesized outputs were then modulated at the carrier frequencies, electronically added

and then the resultant output (identical to Figure 5 but with greater signal to noise) demultiplexed and demodulated by the same circuitry as used in the optical case. Figure 7a shows the experiment corresponding to Figure 6a, the demodulated output of S_1 alone, and with sensor S_2 , S_3 and S_4 also in operation, a ~ 10 mrad rms test signal was used. Again the two traces overlap to the extent that they are indistinguishable, here the noise floor at 1 kHz corresponds to $2 \pm 0.5 \mu\text{rad}/\sqrt{\text{Hz}}$. Figure 7b shows the corresponding crosstalk measurements, again values of less than -60 and -55 dB were achieved for sensor to sensor and array (S_2 , S_3 and S_4) to sensor respectively. A further laboratory demonstration using eight synthesized interferometers in the configuration shown in Figure 8 was performed to ascertain the effect of more channels on the demultiplexing/demodulation technique. The signal input to the demultiplexer/demodulator circuit is shown in Figure 9. The carrier frequencies were between 60 and 88 kHz in this case with a 4kHz spacing between carriers. The results of the experiment corresponding to Figure 6a are shown in Figure 10a. Here the two traces correspond to the output of S_3 with the sensors S_1 through S_8 also in operation; a 10 mrad rms test signal was used. Once again the two traces overlap to the extent that they are indistinguishable, here the noise floor at 1 kHz corresponds to $4 \pm 0.5 \mu\text{rad}/\text{Hz}$. Figure 10b shows the crosstalk measurements for this case; here values of less than -55 dB were achieved for sensor to sensor and array to sensor crosstalk.

Similar measurements in both the optical and synthetic interferometer configuration of sensors S_2 , S_3 and S_4 (through to S_8 for the synthetic case) were made, with results identical to sensor $S_1 \pm 1$ dB. Improved demodulator design will result in $\sim 1 \mu\text{rad}$ noise performance (demonstrated in our laboratory). As all the demodulator circuits (each measuring $3\text{-}1/2 \times 4 \times 4$

cm) were placed without shielding at ~ 4 cm spacing, on an unenclosed circuit card, it is felt that careful design of the demultiplexer/demodulator layout should improve the crosstalk performance.

The detection sensitivity of our present system is limited by $1/f$ laser frequency jitter generated phase-noise. This can easily be reduced by 20-30 dB in the DC to 10 KHz band by using current feedback to the source^{19,20,21}. An improved detectability in the μ rad range would, therefore, be obtainable from individual sensor elements. The shot-noise equivalent phase-shift sensitivity of our set-up was calculated to be $\sim 10^{-7}$ rads/ $\sqrt{\text{Hz}}$, well below that imposed by the phase noise and demodulator. Larger array configurations would, however, due to the additional power splitting and recombination required, suffer a greater shot-noise penalty. Assuming no excess optical loss in the system, and source powers P , the symmetric array of Figure 2 would produce a signal to noise ratio R for sensor (ij) of

$$R_{ij} = \frac{1}{2} \frac{P\gamma}{e} \phi_{ij} N_0^{-3/4} \quad (6)$$

where $N_0 = J^2$ is the total number of sensor elements, and γ is the detector responsivity (A/W).

The shot-noise-equivalent phase shift sensitivity (for $R = 1$) is then

$$\phi_{ij \text{ min}} = 2 \frac{e}{P\gamma} N_0^{3/4} \quad (7)$$

Assuming a source power $P = 10$ mW, a detector responsivity = 0.5 A/W and unity fringe visibility, the dependence of $\phi_{ij \text{ min}}$ due to shot-noise is as shown in Figure 11 for N_0 from 1 to 10^3 . Taking optical loss into account (~ 0.15 dB/splice-coupler) the result is modified only slightly as shown by the upper broken curve in Figure 11; the excess loss has more effect in larger arrays

due to the increased number of couplers and splices required to perform the power splitting and recombination. Also shown in this figure is the variation of the shot noise sensitivity obtainable if all the light from each sensor output is coupled to the detector; in this case $\phi_{ij \text{ min}}$ displays a $N_0^{1/2}$ dependence. This configuration could possibly be implemented by combining the outputs of the single mode fibers with a passive multimode integrated optic chip, the output of which is launched into a multimode fiber. Other noise sources, such as source intensity noise and $1/f$ frequency-jitter induced phase noise will lead to further degradation of ϕ_{min} ; these contributions, however, depend strongly on the channel spacing, laser modulation frequencies and the final demodulation approach adopted.

V. Summary

We have described a simple method of multiplexing and demultiplexing all-optical remote interferometric sensors in the frequency domain using phase generated carriers. The approach requires no increase in circuitry compared to individual sensors employing phase generated carrier demodulation. The array topology using this approach was described and analyzed. For an N_0 sensor array the optimum topology leads to $\sqrt{N_0}$ sources and $\sqrt{N_0}$ fibers to and from the array. Calculation of the shot noise limit for such an approach leads to acceptable noise levels of $1 \mu\text{rad}$ for arrays of hundreds of sensors, with reasonable multiplexing efficiency.

A four element all-fiber array was built and multiplexed. The resultant demodulated output was found to be laser frequency noise limited at $\sim 18 \mu\text{rad}/\sqrt{\text{kHz}}$. The sensor to sensor, and array to sensor crosstalk was found to be less than -60 dB and -55 dB respectively. Measurements with synthesized interferometer outputs gave less than $5 \mu\text{rad}/\sqrt{\text{Hz}}$ noise at 1 kHz for single

sensor, four element array and eight element array operation with similar crosstalk performance. Laser stabilization and improvement in the demodulation design and layout should lead to $\sim 1 \mu\text{rad}$ performance and minimal crosstalk.

Acknowledgement

One of the authors (A. Dandridge) would also like to thank T. G. Giallorenzi and J. H. Cole for discussions in the early stages of this project.

References

1. T.G. Giallorenzi, J.A. Bucaro, A. Dandridge, G.H. Siegel, J.H. Cole, S. C. Rashleigh and R.G. Priest, "Optical Fiber Sensor Tech." IEEE J. Quant. Electron., QE18, 626, 1982.
2. T.G. Giallorenzi and A. Dandridge, "Fiber Optic Sensors: Present and Future," OFS 86, Tokyo, Japan, Oct. 1986.
3. F. Bucholtz, K.P. Koo, A.D. Kersey and A. Dandridge, "Fiber Optic Magnetic Development," SPIE Conf. on Fiber Optics., Boston, MA, Sept. 1986.
4. S.A. Al-Chalabi, B. Culshaw, and D.E.N. Davis, "Partially Coherent Sources in Interferometric Sensors," Proc. of the 1st Int. Conf. on Optical Fibre Sensors, London, April 1983.
5. A. Dandridge and A.B. Tveten, "Phase Noise of Single Mode Diode Lasers in Interferometer Systems," Appl. Phys. Lett., 39, 530, 1981.
6. J.L. Brooks, R.H. Wentworth, R.C. Youngquist, M. Tur, B.Y. Kim and H.J. Shaw, "Coherence Multiplexing of Fiber-Optic Interferometric Sensors," IEEE J. Lightwave Tech., Vol. 3, 1062, 1985.
7. A.D. Kersey and A. Dandridge, "Phase Noise Reduction in Coherence Multiplexed Interferometric Fiber Sensors," Electron. Lett., Vol. 22, 616, 1986.
8. A.D. Kersey and A. Dandridge, "Suppression of Excess Baseband Intensity Noise in Coherence Multiplexed Sensors Using Laser Frequency Modulation Techniques," OFS 86, Tokyo, Japan, Oct. 1986.
9. M.L. Henning, S.W. Thornton, R. Carpenter, W.J. Stewart, J.P. Dakin and C.A. Wade, "Optical Fibre Hydrophones with Down Lead Insensitivity" Proc. of the 1st Int. Conf. on Optical Fibre Sensors, London, April 1983.

10. J.P. Dakin, C.A. Wade, and M.L. Henning, "Novel Optical Fibre Hydrophone Array Using a Single Laser Source and Detector," *Electron. Lett.* 20, 53, 1984.
11. J.L. Brooks, M. Tur, B.Y. Kim, K.A. Fester and H.J. Shaw, "Fiber-Optic Interferometric Arrays with Freedom from Source Phase-Induced Noise," *Opt. Lett.*, Vol. 11, 473, 1986.
12. E.L. Green, G.E. Holmberg, J.C. Gremillion and F.C. Allard, "Remote Passive Phase Sensor," *Optical Fiber Sensor Conf. OFS '85*, San Diego, CA, Feb. 1985.
13. A.D. Kersey, M. Corke, J.D. C. Jones and D.A. Jackson, "Signal Recovery Techniques for Unbalanced Fiber Interferometric Sensors Illuminated by Laser Diodes," *1st Int. Conf. on Optical Fiber Sensors*, Apr. 1983, London, IEE Digest #221, p. 43. Also: G. Economou, R.C. Youngquist and D.E.N. Davies, "Limitations and Noise in Interferometric Systems Using Frequency Ramped Single-Mode Diode Lasers," *IEEE J. of Lightwave Tech.*, Vol. 4, 1601, 1986.
14. I. Sakai, G. Parry and R.C. Youngquist, "Frequency Division Multiplexing of Optical Fibre Sensors Using a Phase/Frequency Modulated Source and Gated Output," *OFS 86*, Tokyo, Japan, Oct. 1986.
15. F. Bucholtz, A.D. Kersey and A. Dandridge, "Multiplexed Nonlinear Interferometric Fiber Sensors," *OFS 86*, Tokyo, Japan, Oct. 1986.
16. A.D. Kersey, F. Bucholtz, K. Sinansky and A. Dandridge, "Interferometric Sensors for DC Measurands - A New Class of Fiber Sensors," *SPIE Conf. on Fiber Optics.*, Boston, MA, Sept. 1986.

17. A. Dandridge, A.B. Tveten and T.G. Giallorenzi, "Homodyne Demodulation Schemes for Fiber Optic Sensors Using Phase Generated Carrier," IEEE J.Quant. Electron., 18, 1047, 1982.
18. A.B. Tveten, A.D. Kersey, E.C. McGarry and A. Dandridge, "Electronic Interferometric Sensor Simulator/Demodulator," OFS'88, New Orleans, LA.
19. A. Dandridge and L. Goldberg, "Current-Induced Modulation in Diode Lasers," Elect. Lett., 18, 302, 1982.
20. F. Favre and E. LeGuen, "High Frequency Stability of Laser Diode for Heterodyne Communication Systems," Electron. Lett., 16, 709, 1980.
21. A. Dandridge and A.B. Tveten, "Electronic Phase Noise Suppression in Diode Lasers," Electron. Lett., 17, 937, 1981.

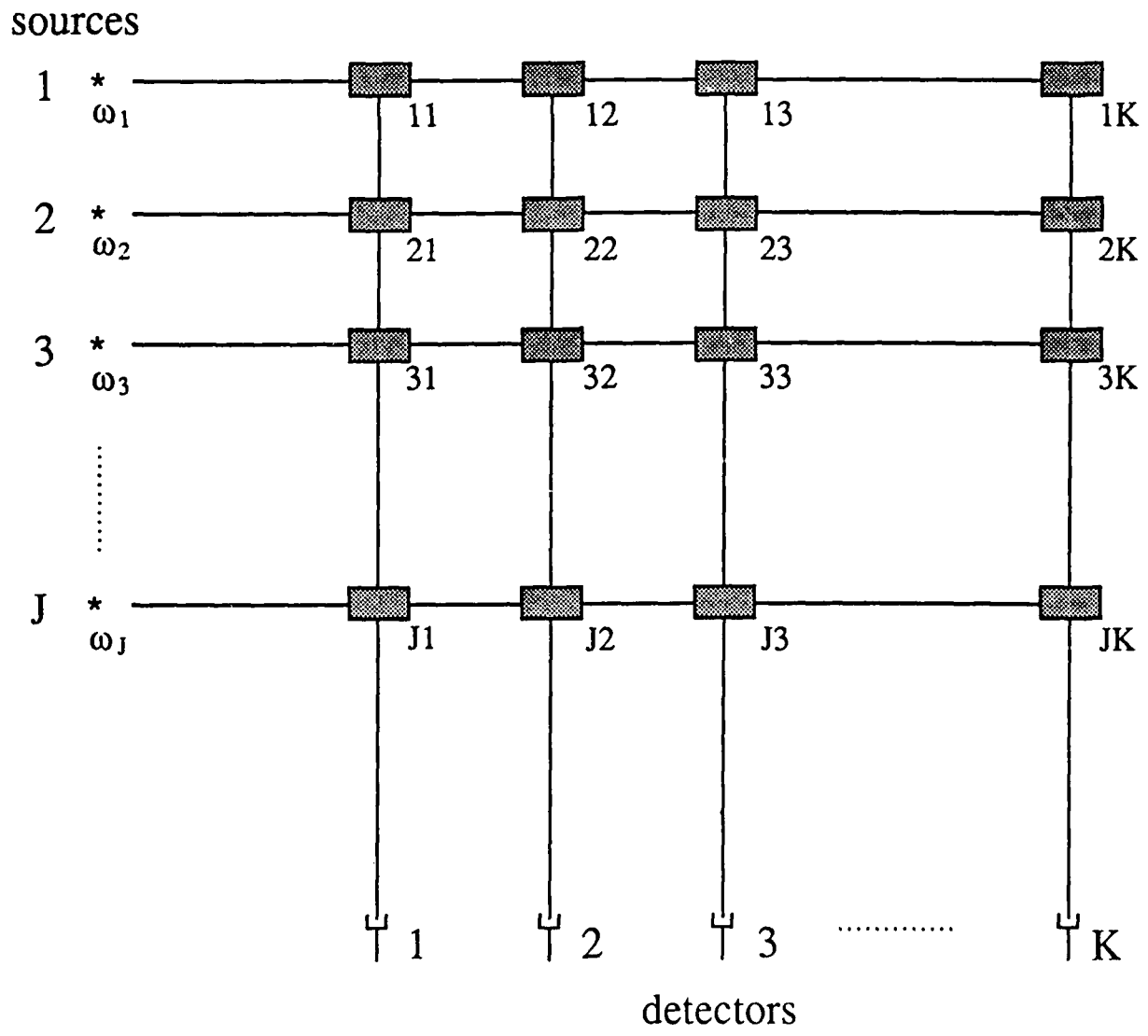


Fig. 1. Matrix representation of the proposed interferometric sensor multiplexing scheme.

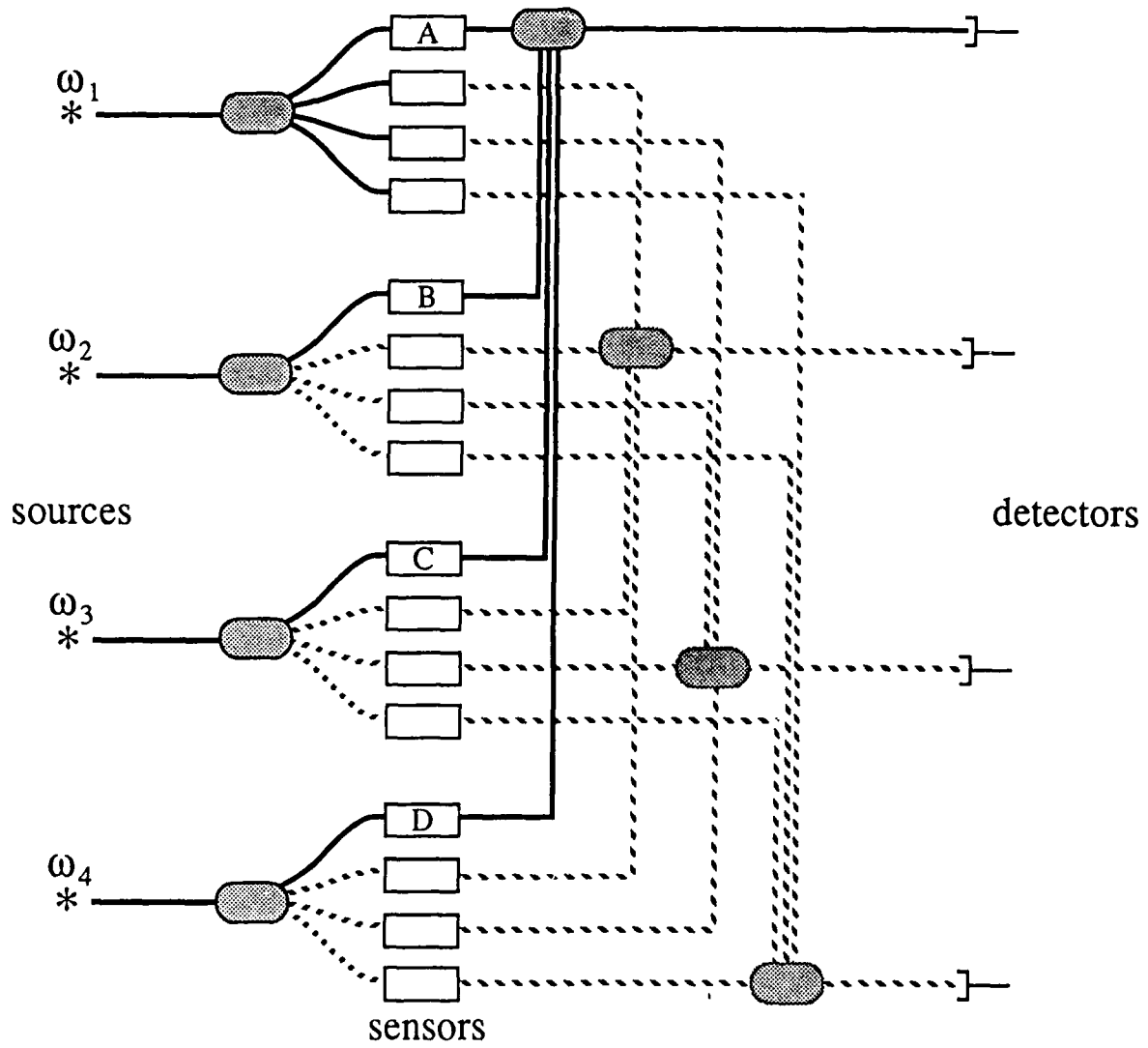


Fig. 2. Optical-fiber 'circuit' for a symmetric 4x4 array.

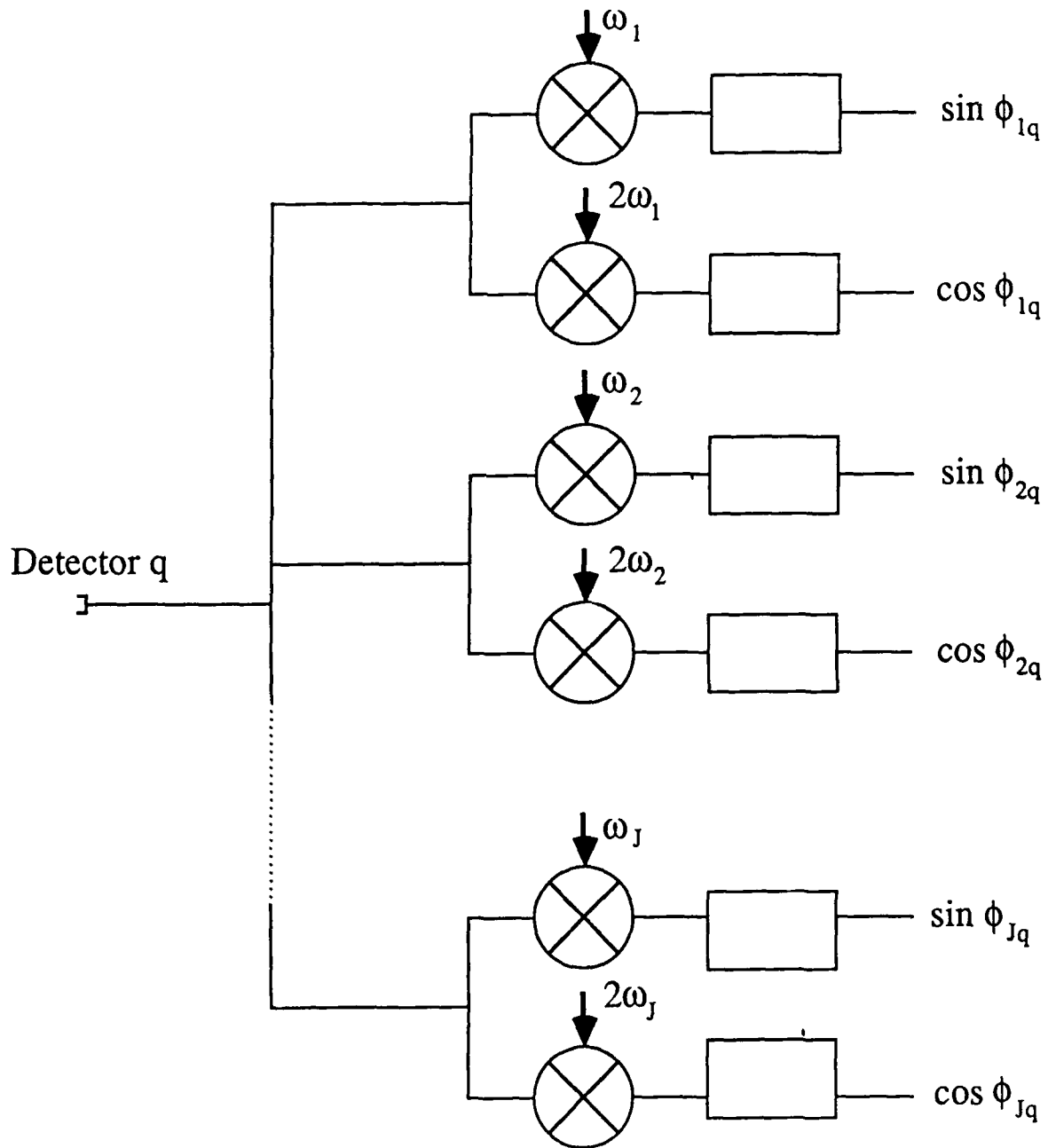
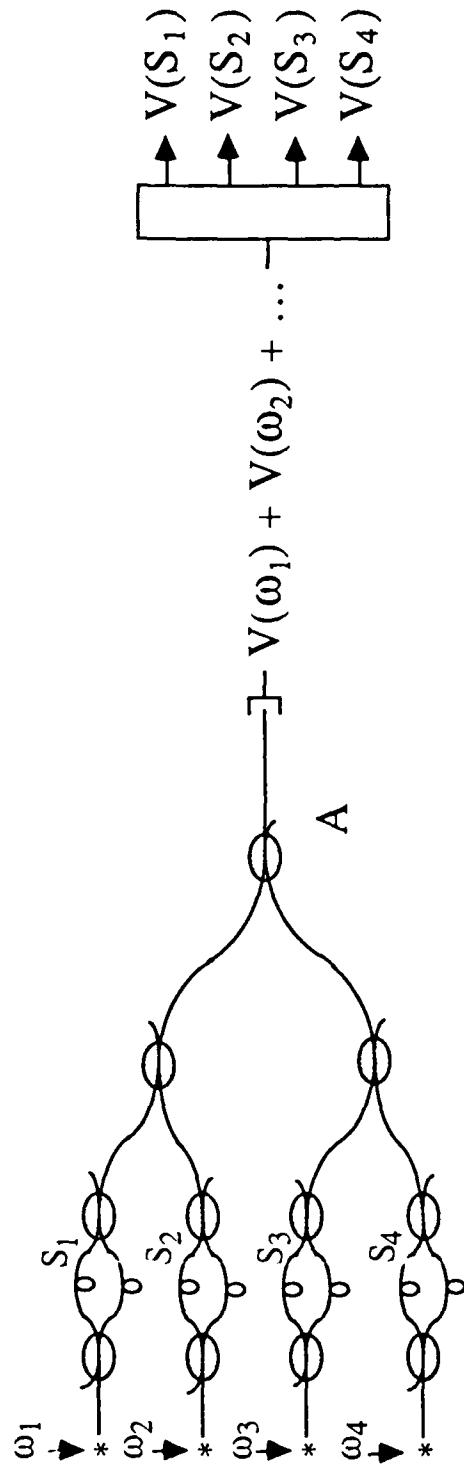


Fig. 3. Schematic of the demultiplexing electronics associated with each (j) detector.



Sensors

Combination

Demultiplexer/Demodulator

Fig. 4. Experimental configuration for sensor multiplexing (combination) and demultiplexing.

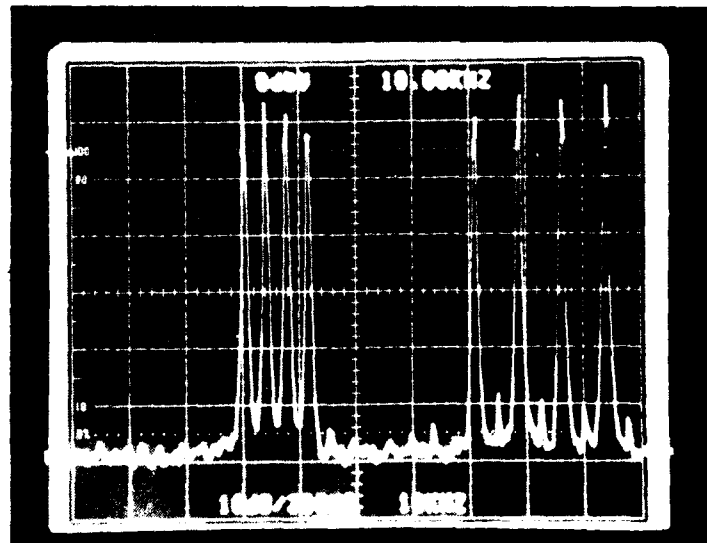
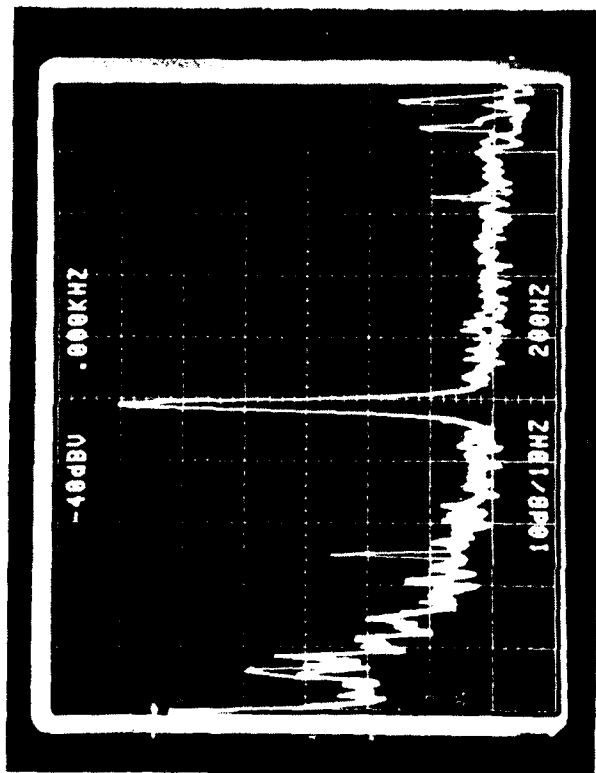
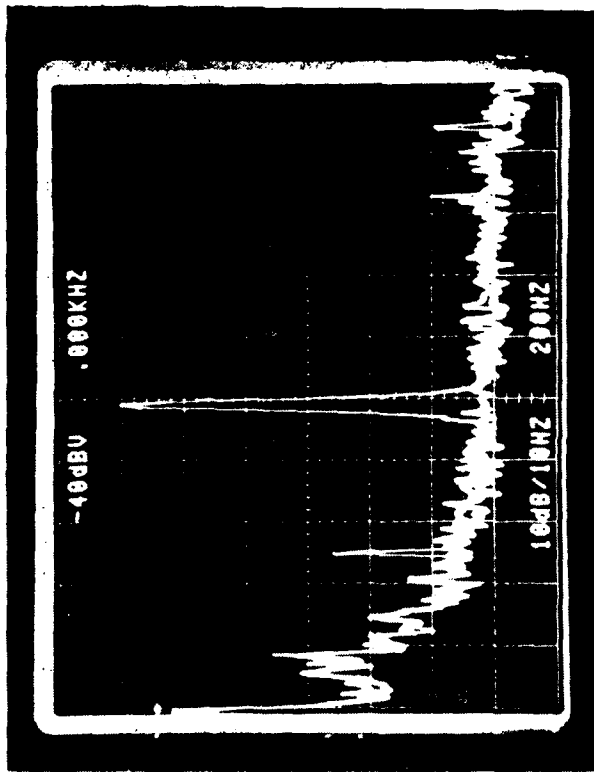


Fig. 5. Amplified output of the photodetector showing four ω components (40, 44, 48 and 52 KHz) and four 2ω components. Trace obtained by multiple spectrum analyzer scan retaining maximum value.



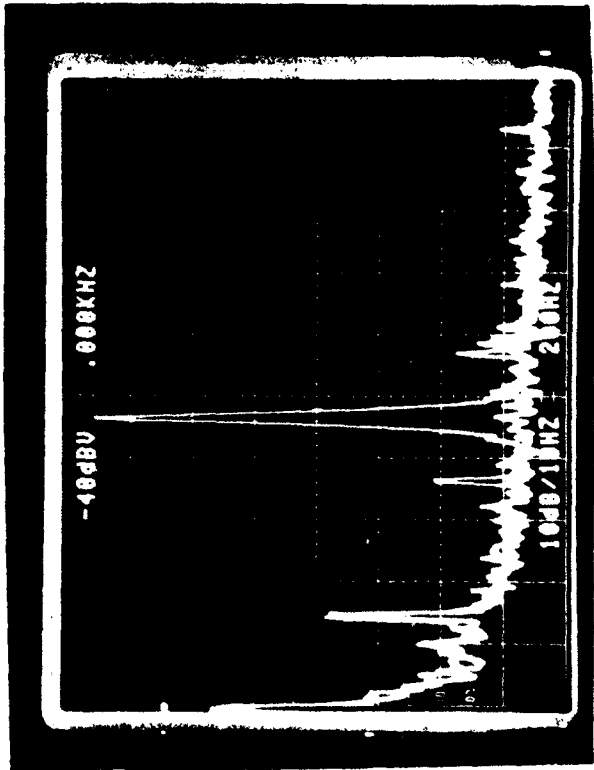
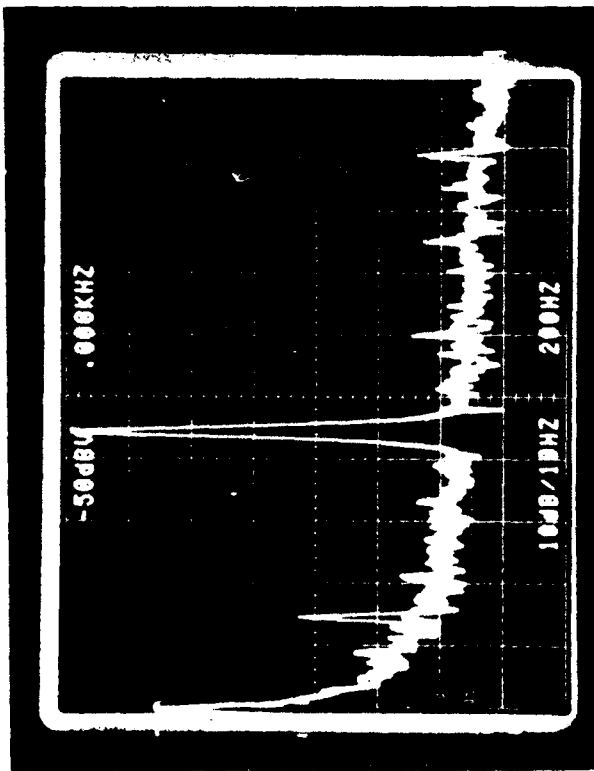
(a)



(b)

Fig. 6. a. Demodulated output of sensor S₁ with a ~ 0.05 rad test signal applied to interferometer, demonstrating a noise floor at 1 KHz of $18 \pm 2 \mu\text{rad}/\sqrt{\text{Hz}}$. Figure shows two traces (overlapping) recorded for S_i operating alone and with four sensors operating indicating a minimal increase in noise.

b. Demodulated output of sensor S₁. Upper trace ~ 0.05 rad test signal applied at 1 KHz, sensors S₂, S₃ and S₄ also in operation. Lower trace, test signal removed from S₁ and applied to S₂, S₃ and S₄ simultaneously demonstrating crosstalk less than -55 dB.



(a)

(b)

Fig. 7. a. Demodulated output of synthetic interferometer S_1 with a ~ 0.01 rad test signal applied to interferometer, demonstrating a noise floor at 1 KHz of $2 \pm 0.2 \mu\text{rad}/\sqrt{\text{Hz}}$. Figure shows two traces (overlapping) recorded for S_1 operating alone and with four sensors operating indicating a minimal increase in noise.

b. Demodulated output of synthetic interferometer S_1 . Upper trace ~ 0.01 rad test signal applied at 1 KHz, sensors S_2 , S_3 and S_4 also in operation. Lower trace, test signal removed from S_1 and applied to S_2 , S_3 and S_4 simultaneously-demonstrating crosstalk less than -55 dB.

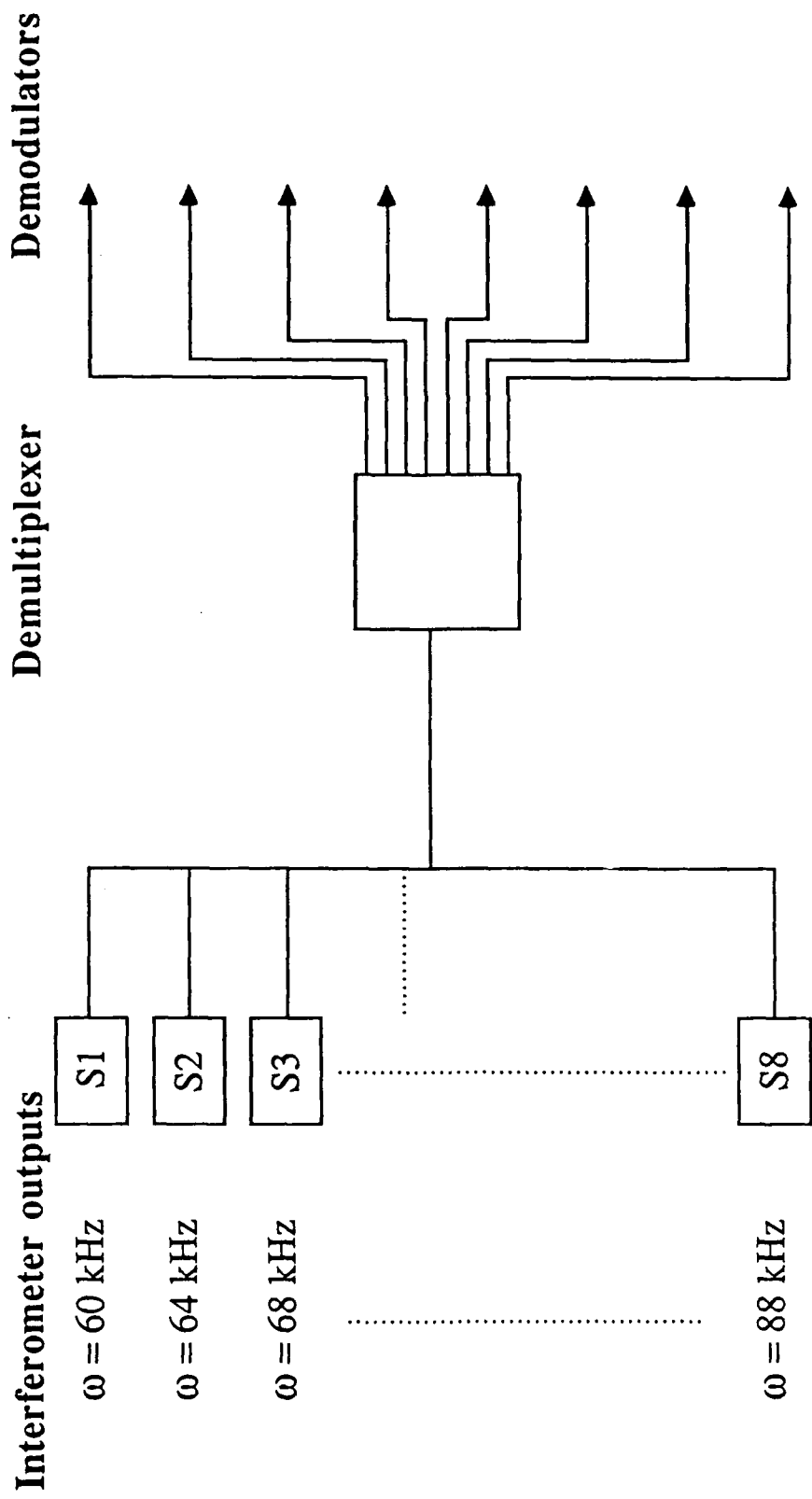
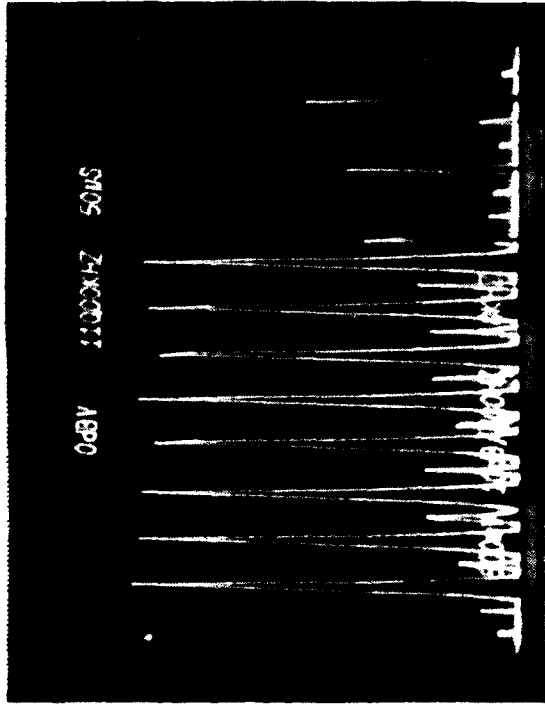


Fig. 8. Experimental configuration for eight channel demultiplexer/demodulator demonstration.

2 ω terms



ω terms

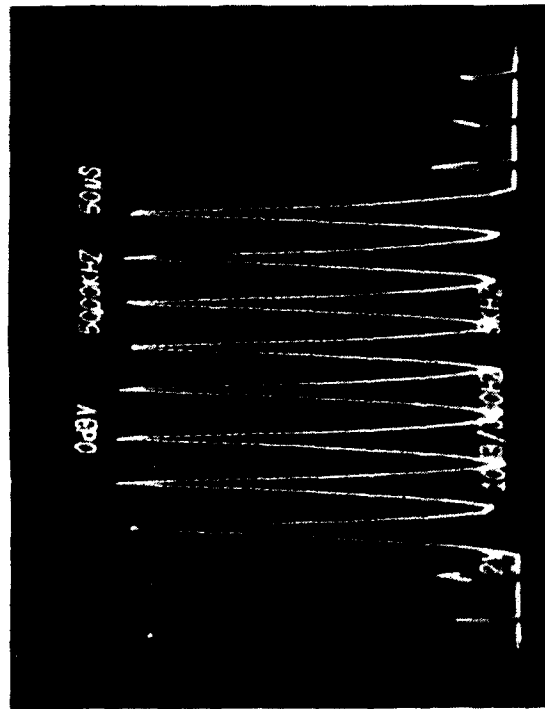
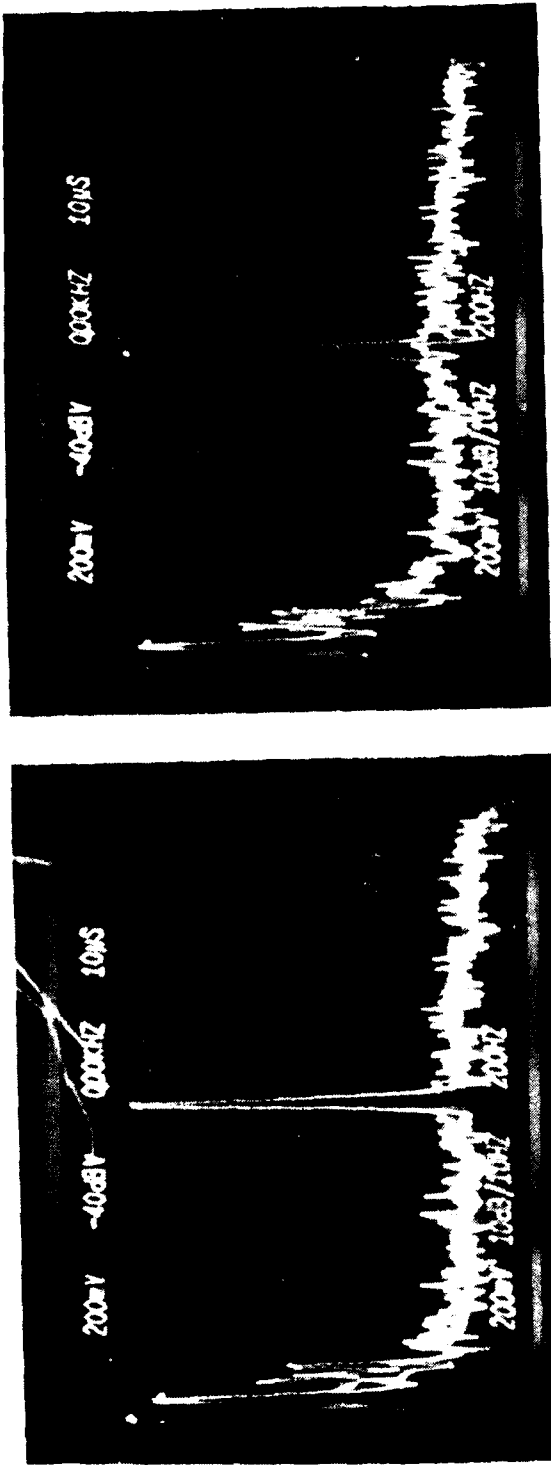


Fig. 9. Input signal to the demodulator showing eight ω components and eight 2ω components. Trace obtained by multiple spectrum analyzer scan retaining maximum value.



(a)

Fig. 10. a) Demodulated output of synthetic interferometer S₃ with a ~ 10 mrad test signal applied to interferometer, demonstrating a noise floor at 1 kHz of 4 + 0.5 μrad/√Hz. Figure shows two traces (overlapping) recorded for S₃ operating alone and with eight sensors operating indicating a minimal increase in noise.

(b)

b) Demodulated output of synthetic interferometer S₃. Upper trace 10 mrad test signal applied at 1 kHz, other sensors S₁ - S₈ also operation. Lower trace, test signal removed from S₃ and applied to other sensors S₁-S₈ simultaneously, demonstrating crosstalk less than -55 dB.

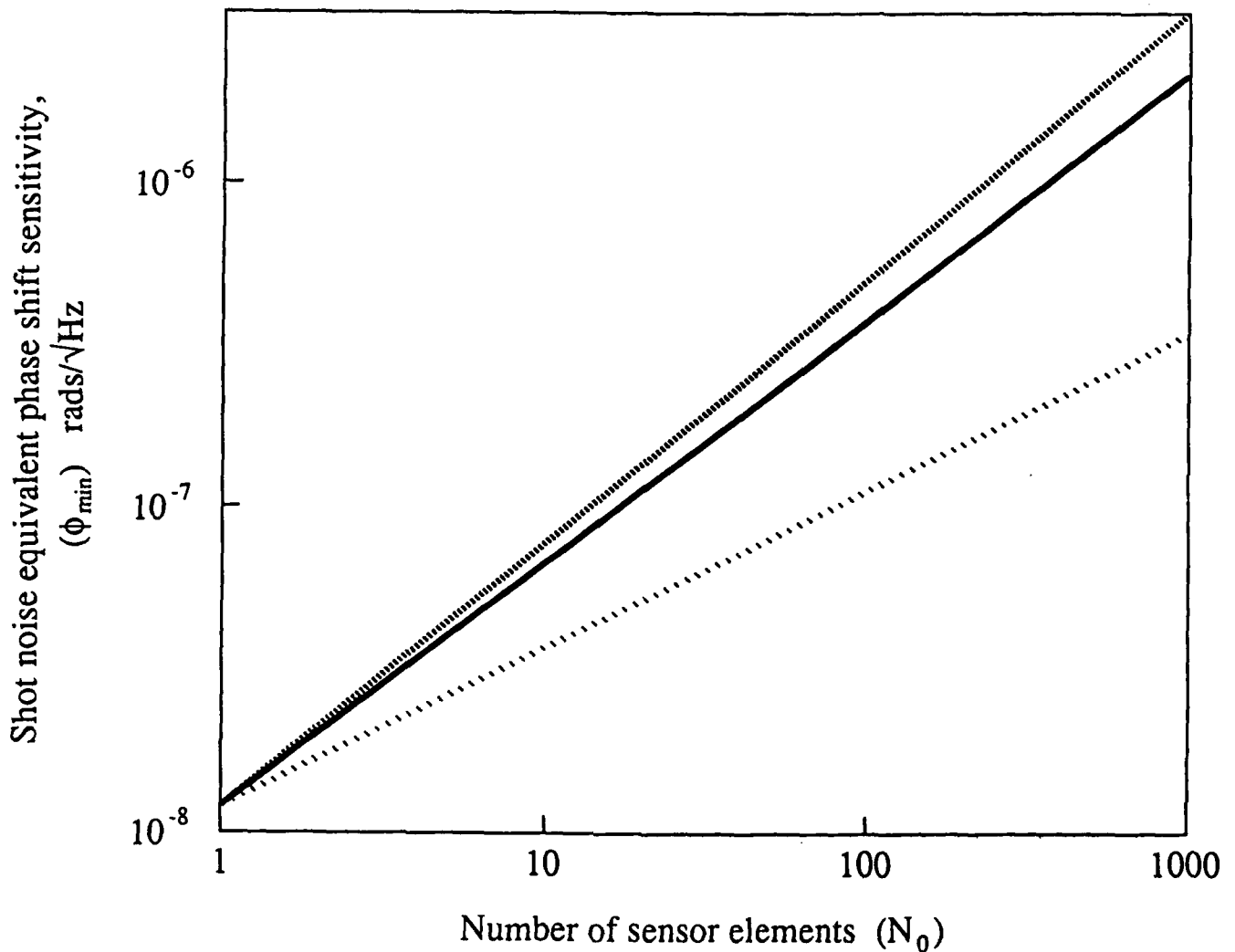


Fig. 11. Shot-noise equivalent phase-shift sensitivity (ϕ_{\min}) as a function of N_0 . Note: calculation assumes a symmetric array only, i.e. $N_0 = J^2$ (J integer) and 10 mW source powers. Solid line indicates lossless system; upper broken line indicates result with 0.15 dB loss/(splice/coupler); lower broken curve indicates shot noise sensitivity obtainable if all the light from each sensor output is coupled to the detector (i.e. avoiding the intrinsic loss in recombination: e.g., -3 dB for each 2x2 coupler).